

On the use of complex susceptibility data to complement magnetic viscosity measurements

P C Fannin†, S W Charles‡ and T Relihan†

† Department of Microelectronics and Electrical Engineering, Trinity College, Dublin 2, Ireland

‡ Department of Chemistry, University College of North Wales, Bangor LL57 2UW, UK

Received 16 August 1993, in final form 21 October 1993

Abstract. Magnetic viscosity measurements consist of placing an ensemble of small magnetic particles in a very large magnetic field, which tends to align the magnetic moments, m_p , of the particles in the direction of the field and then observing the decay, with time, of the magnetization when the field is removed. In measuring the magnetic viscosity, it is possible for magnetization data to be unavoidably lost due to the time delay between removing the applied field and making the first magnetization measurement. It is shown that, by taking the inverse Fourier transform of the frequency-dependent complex susceptibility, $\chi(\omega) = \chi'(\omega) - i\chi''(\omega)$, of the sample, it is possible to recover data corresponding to that which would have been measured during the period of the time delay.

1. Introduction

Magnetic viscosity measurements consist of placing an ensemble of small magnetic particles, such as a ferrofluid sample, in a very large magnetic field, which tends to align the magnetic moments, m_p , of the particles in the direction of the field and then observing the decay, with time, of the magnetization, $M_r(t)$, when the field is removed.

$M_r(t)$ is approximately given by

$$M_r(t) = M_r(0)e^{-t/\tau} \quad (1)$$

where $M_r(0)$ is the remanent magnetization at some arbitrary time taken as $t = 0$ and τ is the average relaxation time of the particles. This phenomenon is usually referred to as magnetic viscosity because of the manner in which the measurements are made. Because of the nature of the magnetic viscosity measurements, they do not start at time $t = 0$ [1–3], resulting in the magnetization decaying during removal of the field. Thus magnetization data corresponding to the contribution of the magnetic moments relaxing during this time, through either Néel [4–6] or Brownian [7] relaxation mechanisms, are lost. Both these mechanisms are applicable in the case of a ferrofluid, whilst, in the case of a solid matrix, relaxation is by the Néel mechanism only.

A distribution of relaxation times is associated with a distribution of particle sizes and anisotropy constants,

therefore it is not likely that one exponent is sufficient to describe the process, unless the distribution is extremely narrow. It is reported [8] that the experimental data in terms of $M_r(t)$ are better described by a $\ln(t)$ dependence with

$$M_r(t) = C - S \ln(t). \quad (2)$$

However, this expression does not reflect the nonlinear behaviour of a number of systems [9, 10] and it has been shown that this behaviour is governed by the distribution of energy barriers of the magnetic moments within the system. It has a further limitation in that the average relaxation time, τ , of the system, which is of interest, is incorporated into the constant C in equation (2). Aharoni [11] is very critical of the use of this function which he says 'is so unphysical and so inconvenient to use or to interpret' (*sic*). Indeed, unlike equation (1), which can be extended to measurements at time $t = 0$, equation (2) diverges for both very short and very long times [12]. In order to incorporate a distribution of relaxation times in equation (1), Aharoni uses, for convenience, a Γ distribution function so that integration of the expression can be carried out analytically. This Γ function contains two adjustable parameters, which contain all the physical information necessary to characterize the particle distribution [13]. He also suggests an alternative method of determining τ , which involves measuring the AC magnetic susceptibility, $\chi(\omega)$, of the particles of the magnetic viscosity region. Provided that it is known where to look, a maximum in the $|\chi(\omega)|$ versus frequency plot should be observed similar to that

reported in [14] for very low temperatures, which would enable an average relaxation time to be determined. This method presupposes that the distribution is sufficiently narrow that the loss-peak maximum is not smeared out.

In the study of ultra-fine, single-domain magnetic particles, as used for example in magnetic fluids, Fannin *et al* [15, 16], have used measurements of the complex magnetic susceptibility, $\chi(\omega)$, to determine an average relaxation time of the magnetic moments in almost zero magnetic field. Such measurements have been performed on fluids with packing fractions as low as 0.007. Measurements have also been made over the frequency range 10 Hz to 1 GHz [17]; a very much greater number of decades than that employed in magnetic viscosity measurements, which, in the case of particulate systems, have generally been made on large (tape) particles where the relaxation times are many orders of magnitude longer.

In this study, it is shown that, by determining the inverse Fourier transform (IFT) of the complex susceptibility components, $\chi'(\omega)$ and $\chi''(\omega)$, respectively, it is possible to proceed from the frequency domain to the time domain and generate the corresponding decay curve, not only over many decades of time but for starting times equivalent to nanoseconds in the corresponding magnetic viscosity measurements.

2. Complex susceptibility

The theory developed by Debye [18] to account for the anomalous dielectric dispersion in dipolar fluids has been used [16, 19] to account for the analogous case of magnetic fluids. Debye's theory holds for spherical particles when the magnetic dipole-dipole interaction energy, U , is small relative to the thermal energy kT . The complex frequency-dependent magnetic susceptibility, $\chi(\omega)$, may be written in terms of its real and imaginary components, where

$$\chi(\omega) = \chi'(\omega) - i\chi''(\omega). \quad (3)$$

According to Debye's theory the complex susceptibility, $\chi(\omega)$, has a frequency-dependence given by the equation

$$\chi(\omega) = \chi_\infty + (\chi_0 - \chi_\infty)/(1 + i\omega\tau) \quad (4)$$

where χ_0 and χ_∞ indicate the values of susceptibility at $\omega = 0$ and at very high frequencies, respectively. τ is the effective relaxation time with

$$\tau = 1/\omega_m = 1/(2\pi f_m) \quad (5)$$

where f_m is the frequency at which $\chi''(\omega)$ is a maximum.

Equation (4) is often written as

$$(\chi(\omega) - \chi_\infty)/(\chi_0 - \chi_\infty) = 1/(1 + i\omega\tau). \quad (6)$$

To develop the relationship between the frequency-domain components, $\chi(\omega)$, of the magnetic sample and

its time-domain counterpart, it is necessary to review the procedure by which equation (6) is derived [20].

Consider the situation where a small DC field, H_1 , is instantaneously applied to a system that is in equilibrium in a larger DC field, H . This results in a rise transient, $M(t)$, of the approximate form

$$M(t) = (\chi_0 - \chi_\infty)[1 - \exp(-t/\tau)]H_1. \quad (7)$$

For a linear system, the decay transient that follows instantaneous removal of H_1 is the mirror image of the rise transient, with an after-effect function, $f(t)$, of

$$f(t) = (\chi_0 - \chi_\infty)[\exp(-t/\tau)]. \quad (8)$$

It is readily shown [20, 21] that the frequency-dependent susceptibility arising from application of an AC field, $H_1 \exp(-i\omega t)$, is given by

$$(\chi(\omega) - \chi_\infty) = - \int_0^\infty \frac{d(f(t))}{dt} \exp(i\omega t) dt \quad (9)$$

and integrating by parts to obtain

$$\begin{aligned} \frac{\chi(\omega) - \chi_\infty}{\chi_0 - \chi_\infty} &= \left(1 - i\omega \int_0^\infty \exp(-t/\tau) \exp(-i\omega t) dt \right) \\ &= 1/(1 + i\omega\tau) \end{aligned} \quad (10) \quad (11)$$

the Debye equation. However, the integral of equation (9) is, by definition, the Fourier transform of the function $-d(f(t))/dt$, which can thus be obtained by taking the IFT of equation (9). Having determined $[-d(f(t))/dt]$, we have from equations (8) and (1)

$$\begin{aligned} -(\tau/f(0))[d(f(t))/dt] &= f(t)/f(0) \\ &= \exp(-t/\tau) = M_r(t)/M_r(0) \end{aligned} \quad (12)$$

where $f(0) = (\chi_0 - \chi_\infty)$.

Equation (12) shows that the normalized plots of the IFT of $\chi(\omega)$ and of the magnetization are equivalent, thus confirming that the technique presented is capable of determining magnetic viscosity data.

3. The Fourier transform

The Fourier transform, $F(\omega)$, of a continuous function, $f(t)$, is defined as

$$F(\omega) = \int_{-\infty}^\infty f(t) \exp(-i\omega t) dt \quad (13)$$

and its inverse function as

$$f(t) = \frac{1}{2\pi} \int_{-\infty}^\infty F(\omega) \exp(i\omega t) d\omega. \quad (14)$$

As an example, consider the case where $f(t)$ is a one-sided exponential pulse $A \exp(-t/\tau)$. From equation (13), the Fourier transform of $f(t)$ is

$$F(\omega) = A\tau/(1 + i\omega\tau) \quad (15)$$

which has the same form as equation (11), the Debye equation. So, immediately it is known that the IFT of $\chi(\omega)$ should be an exponential function of form $A \exp(-t/\tau)$. In reality $\chi(\omega)$ is not a continuous function but a sampled function and so the discrete Fourier transform (DFT) must be used.

If the number of samples is of the power of two then the DFT may be implemented using the fast Fourier transform (FFT) algorithm. Where $\chi(\omega)$ consists of N samples, implementation of the FFT requires approximately $N \log_2 N$ operations. The FFT technique is employed here.

In a practical measurement, $\chi'(f)$ and $\chi''(f)$ are measured at evenly spaced intervals, Δf Hz, from a start frequency of Δf Hz to a frequency f_∞ Hz; the latter being the frequency at which χ_∞ is deemed to have been reached. Also, the start frequency must be equal to or a multiple of the incremental frequency. The proposed technique also assumes that the zero-frequency data are the same as that obtained at the first measurement point.

Furthermore, since FFT techniques require the signal to be transformed to be periodic, the negative of $\chi'(f)$ and $\chi''(f)$ from 0 to $-f_\infty$ Hz must be generated. This is a simple matter since $\chi'(f)$ and $\chi''(f)$ are even and odd functions of f and are easily implemented in software.

A factor that should be considered when choosing the incremental measurement frequency Δf and the final frequency f_∞ is the fact that the limits of integration of the integral in equation (13) are $\pm\infty$. In practice this is limited to $\pm f_\infty$, which is equivalent to multiplying $\chi'(f)$ by a rectangular window. Other types of windows, such as Hamming or triangular, may be used in order to minimize the effects of the rectangular window.

4. Application of the IFFT transform

To test the validity of the proposed technique, it was first applied to theoretical Debye curves, where one knew (from equation (15)) what the resultant IFFT should be. It was then tested on data obtained in a dynamic situation.

Initially, equation (6), with $\chi_0 = 1$ and $\chi_\infty = 0$, was plotted for a maximum $\omega = 5 \times 10^8$ rad s⁻¹, $N = 8192$ points and $\omega_m = 10^6$ rad s⁻¹, and the corresponding Debye plots of $\chi'(\omega)$ and $\chi''(\omega)$ as shown in figure 1. The corresponding transform plot of $f(t)$ against time is shown in figure 2(a) and it is found to be of the exponential form predicted. One notes that its magnitude falls to 1/e of its peak value in a time of τ s. This corresponds to the time constant $\tau = 1/\omega_m$, thus establishing the fact that the 'time-constant-time' of the IFFT corresponds to the average relaxation time of the particles under examination. Figure 2(b) shows the result for the case where $\chi_\infty = 0.2$ with the time constant the same as in the previous case. This is as expected since τ is a function of ω_m , which remains unchanged. Figure 2 also displays some slight distortion at $t \approx 0$ (as highlighted by the inset to figure 2). This effect arises because ω does not go to infinity but is

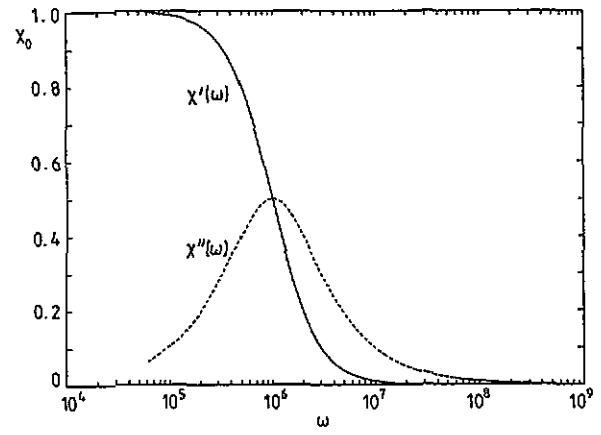


Figure 1. Plot of $\chi'(\omega)$ and $\chi''(\omega)$ against ω (rad s⁻¹) for the Debye case with $\chi_\infty = 0$ and $n = 8192$ points.

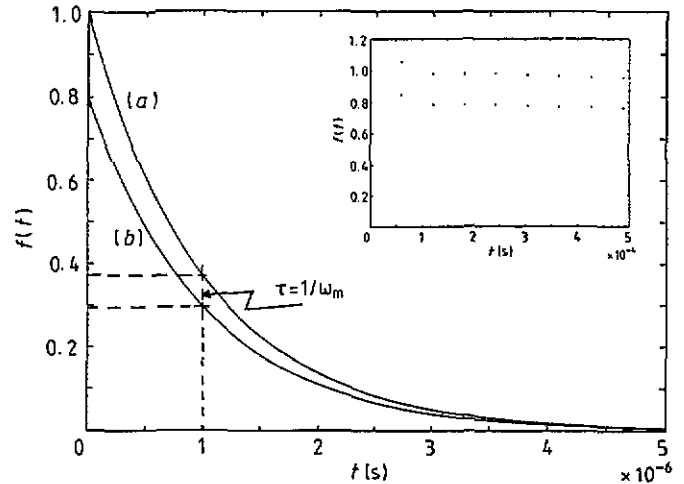


Figure 2. (a) Plot of $f(t)$ against t (s) for the Debye case with $\chi_\infty = 0$, and (b) plot of $f(t)$ against t (s) for the Debye case with $\chi_\infty = 0.2$. The inset illustrates the distortion in $f(t)$ as t approaches zero.

truncated at $\omega = 5 \times 10^8$ rad s⁻¹, which corresponds to a time of 1.26×10^{-8} s.

The technique was then applied to a profile having two absorption peaks occurring at ω_{m1} and ω_{m2} , corresponding to approximately 10^5 and 1.8×10^7 rad s⁻¹ respectively, as illustrated in figure 3. This profile, which has two distinct slopes in the $\chi'(\omega)$ plot, can be described by the expression

$$\chi(\omega) = \chi_{\infty 2} + (\chi_0 - \chi_{\infty 1}) / (1 + i\omega\tau_1) + (\chi_{\infty 1} - \chi_{\infty 2}) / (1 + i\omega\tau_2) \quad (16)$$

where $\omega_{m1} = 1/\tau_1$ and $\omega_{m2} = 1/\tau_2$.

Now the IFFT of equation (16), $v(t)$, has the approximate form

$$v(t) = (1/\tau_1)(\chi_0 - \chi_{\infty 1}) \exp(-t/\tau_1) + (1/\tau_2)(\chi_{\infty 1} - \chi_{\infty 2}) \exp(-t/\tau_2) \quad (17)$$

so, provided that ω_{m1} and ω_{m2} are well separated, $v(t)$ should display two distinct exponential curves.

The log-linear plot of figure 4(a) shows the result of transforming the data of figure 3. It clearly shows

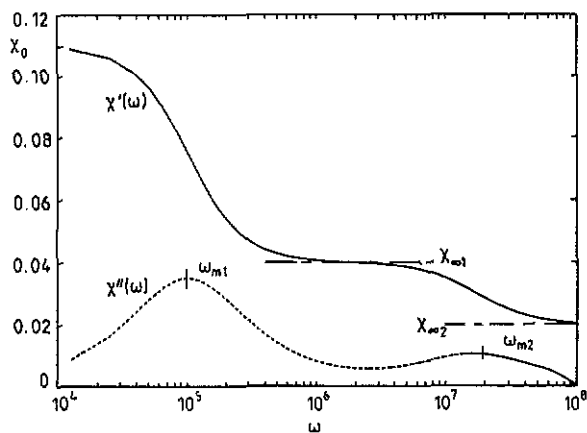


Figure 3. Plot of $\chi'(\omega)$ and $\chi''(\omega)$ against ω (rad s^{-1}) for the double-Debye case with loss-peaks at $\omega_{m1} = 10^5 \text{ rad s}^{-1}$ and $\omega_{m2} = 17.8 \times 10^6 \text{ rad s}^{-1}$, respectively.

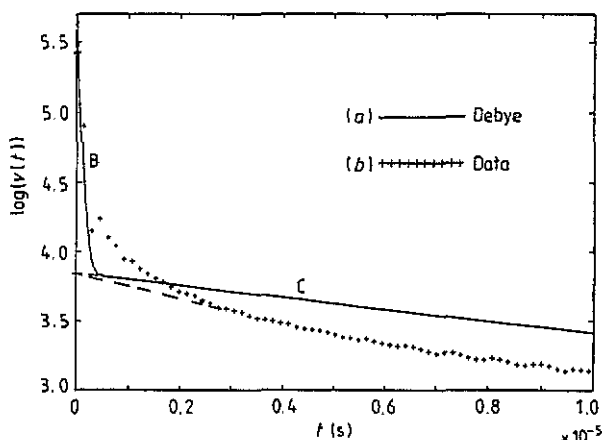


Figure 4. (a) Plot of $\log(v(t))$ against t (s) for the double-Debye case of figure 3. (b) Plot of $\log(v(t))$ against t (s) for the data of figure 5.

the two distinct decaying exponentials, B and C, which intercept the y axis at approximate values of $\log(5.55)$ and $\log(3.85)$ respectively, as determined by equation (17) with $(\chi_{\infty 1} - \chi_{\infty 2}) = 0.02$ and $(\chi_0 - \chi_{\infty 1}) = 0.07$.

Having established that the technique was successful with theoretically generated data, it was then applied to susceptibility data obtained for a ferrofluid consisting of a colloidal suspension of single-domain magnetite particles of volume fraction $\eta = 0.01$, with a log-normal volume distribution of median diameter of 12.1 nm and a standard deviation of 0.51 dispersed in a water carrier.

Measurements were performed over the frequency range 400 Hz to 3.28 MHz in steps of 400 Hz and the resulting plots of $\chi'(\omega)$, $\chi''(\omega)$ are shown in figure 5, with a first loss-peak of $\chi''(\omega)$ occurring at $\omega_{m1} = 10^5 \text{ rad s}^{-1}$, and an incomplete second peak at approximately $\omega_{m2} = 1.8 \times 10^7 \text{ rad s}^{-1}$ (highlighted in the inset of figure 5). These parameters correspond to those chosen in the theoretical example of figure 3 and enable a comparison to be made between its transformation, figure 4(b), and the Debye transformation shown in figure 4(a). It should be noted that the ferrofluid sample consists of a distribution of particle sizes and hence a distribution of relaxation times, whilst the theoretical case consists of only

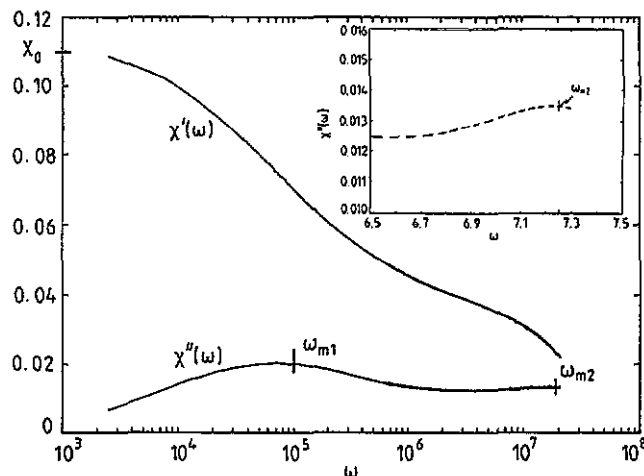


Figure 5. Plot of $\chi'(\omega)$ and $\chi''(\omega)$ against ω (rad s^{-1}) for a colloidal suspension of magnetite particles (of volume fraction $\eta = 0.01$, with median diameter of 12.1 nm and standard deviation of 0.51) dispersed in water, with two loss-peaks at $\omega_{m1} = 10^5 \text{ rad s}^{-1}$ and $\omega_{m2} = 17.8 \times 10^6 \text{ rad s}^{-1}$ respectively. The inset shows highlights of data centred on ω_{m2} .

two relaxation times represented by two Debye-type profiles; this fact being manifest by (i), the difference in slopes of the corresponding $\chi'(\omega)$ curves and (ii), no longer are the log-linear plots for the two exponential profiles linear, reflecting the presence of a distribution of relaxation times. Notwithstanding these differences between theoretical and dynamic profiles, the similarity between the corresponding transformed wave forms is quite satisfactory, with the lower frequency exponential cutting the y axis at almost the same point as its theoretical counterpart, whilst the second exponential intersects at approximately $\log(5.5)$, compared with the theoretical intercept of $\log(5.55)$.

5. Conclusion

The relationship between the complex susceptibility and the magnetic viscosity of a system of single-domain particles has been presented. It has been demonstrated, both in a theoretical and in a practical situation, that the use of FFT techniques enables one to process data, measured in the frequency domain, to generate data in the time domain; data that were unmeasurable directly in the time domain. Here we have effectively performed the equivalent time measurement over the approximate range $0.3 \times 10^{-6} - 2.5 \times 10^{-3} \text{ s}$; a time region outside that possible with current magnetic-viscosity measurement techniques.

Several papers have been published by the authors on measurement of the complex susceptibility of ferrofluids [15–17]; however, this is the first time that they have reported on the application of such measurements to determine time-domain equivalent data.

The authors have recently reported [16] on automated susceptibility measurements over the frequency range 10 Hz to 1 GHz, corresponding to a dynamic range of eight decades of magnetization. To the authors'

knowledge, the current lower frequency limit of commercially available, suitable automated measuring equipment is 5 Hz. Should future developments result in this lower limit being reduced towards a frequency of 10^{-4} Hz, which is currently available for automated dielectric measurements, then this would enable the potential of the technique presented to be fully utilized in extending time measurements to the usual magnetic-viscosity measurement domain.

Acknowledgments

We thank the EC for financial support under the BRITE-EURAM programme and Yu P Kalmykov for helpful discussions.

References

- [1] Aharoni A 1992 *Phys. Rev. B* **46** 5434
- [2] Charap S H 1988 *J. Appl. Phys.* **63** 2054
- [3] Schwartz A J and Soffa W A 1990 *IEE Trans. Magn.* **26** 1816
- [4] Neel L 1949 *Ann. Geophys.* **5** 99
- [5] Brown W F 1963 *Phys. Rev.* **130** 1677
- [6] Bessais L, Jaffel L Ben and Dormann J L 1992 *Phys. Rev. B* **45** 7805
- [7] Brown W F 1963 *J. Appl. Phys.* **34** 1319
- [8] Street R and Woolley J C 1949 *Proc. Phys. Soc. A* **62** 562
- [9] Chamberlin R V, Mozurkerwich G and Orbach R 1984 *Phys. Rev. Lett.* **52** 867
- [10] Yeung I, Ruan W and Roshko R M 1988 *J. Magn. Magn. Mater.* **74** 59
- [11] Aharoni A 1992 *Phys. Rev. B* **46** 5434
- [12] Aharoni A 1992 *Proc. Studies of Magnetic Properties of Fine Particles and their Relevance to Materials Science* (Amsterdam: North-Holland)
- [13] Aharoni A 1985 *J. Appl. Phys.* **57** 4702
- [14] Awschalom D D, McCord M A and Grinstein L 1990 *Phys. Rev. Lett.* **65** 783
- [15] Fannin P C, Scaife B K P and Charles S W 1986 *J. Phys. E: Sci. Instrum.* **19** 23
- [16] Fannin P C, Charles S W and Relihan T 1993 *Meas. Sci. Technol.* **4** 1160-2
- [17] Fannin P C, Scaife B K P and Charles S W 1988 *J. Magn. Magn. Mater.* **72** 95
- [18] Debye P 1929 *Polar Molecules* (New York: The Chemical Catalogue Company)
- [19] Maiorov M M 1979 *Magnetohydrodynamics* **2** 21
- [20] Coffey W T, Kalmykov Yu P and Clegg P J 1992 On the theory of the Debye and Néel relaxation of single domain ferromagnetic particles *Advances in Chemical Physics* vol 83 (New York: Wiley) p 264
- [21] Scaife B K P 1989 *Principles of Dielectrics* (London: Oxford Science)